

# Zinc Carboxylate Functionalized Mesoporous SBA-15 Catalyst for Selective Synthesis of Methyl-4,4'-di(phenylcarbamate)

Xingcui Guo · Zhangfeng Qin · Weibin Fan ·  
Guofu Wang · Ruihua Zhao · Shaoyi Peng ·  
Jianguo Wang

Received: 4 August 2008 / Accepted: 4 November 2008 / Published online: 4 December 2008  
© Springer Science+Business Media, LLC 2008

**Abstract** Mesoporous SBA-15 functionalized with zinc carboxylate (ZC/SBA-15) was used as a heterogeneous catalyst for the selective synthesis of methyl-4,4'-di(phenylcarbamate) (MDC) from dimethyl carbonate (DMC) and 4,4'-methylenedianiline (MDA). ZC/SBA-15 was prepared in three steps: first, SBA-15 grafted with –CN group was synthesized via the conventional one-pot route; then the –CN group was converted into –COOH group in H<sub>2</sub>SO<sub>4</sub> solution; lastly, Zn<sup>2+</sup> ions were introduced into the material by a facile ion-exchange process. The catalyst ZC/SBA-15 exhibits high MDA conversion (near 100%) and MDC selectivity (about 86.5%) with good recyclability in the MDC synthesis; this may provide a new approach for the non-phosgene synthesis of isocyanates.

**Keywords** SBA-15 · Zinc carboxylate · Functionalization · Methoxycarbonylation · Methyl-4,4'-di(phenylcarbamate) · Dimethyl carbonate · 4,4'-Methylenedianiline

## 1 Introduction

Aromatic isocyanates are of great commercial importance in the manufacture of polyurethanes and herbicides [1].

Among them, diphenylmethane-4,4'-diisocyanate (MDI) has been particularly well developed to produce tough elastomers and flexible foams. Conventionally, MDI is synthesized from aromatic amines with highly toxic and corrosive phosgene [2]. To avoid using phosgene, several alternative methods for producing MDI have been proposed [3]. Among these methods, thermal decomposition of methylene-4,4'-di(phenylcarbamate) (MDC) to obtain MDI is very attractive [4], because MDC can be efficiently synthesized by non-phosgene methods like reductive carbonylation of aromatic nitro compounds [5], oxidative carbonylation of amines [6], methoxycarbonylation of 4,4'-methylenedianiline (MDA) with dimethyl carbonate (DMC) [7, 8]. The last method employs environmentally benign materials and mild reaction conditions and then has attracted many attentions in recent years. For the synthesis of carbamates from dialkyl carbonate and amines, Pb(OAc)<sub>2</sub> [9], Zn(OAc)<sub>2</sub> [10], Yb(OTf)<sub>3</sub> hydrate [11] and Zn(OAc)<sub>2</sub>/AC [12] have been used as catalysts. However, these catalysts are easily dissolved in the reaction media, which may bring on problems in product separation and catalyst recovery.

On the other side, metal and nonmetal catalysts bound to the surface of mesoporous materials have received considerable attention in organic synthesis because of their environmental compatibility, reusability, high selectivity and simplicity in operation [13–16]. Carloni et al. [17] prepared a hybrid organic-inorganic material MCM-41-TBD by anchoring 1,5,7-triazabicyclo[4.4.0]dec-5-ene (TBD) to MCM-41 silica, which exhibited high catalytic activity in the synthesis of carbamates or unsymmetrical alkyl carbonates through the reaction of diethyl carbonate with aliphatic amines or alcohols. The solid catalyst could be recovered simply by filtration and reused for many cycles without losing its activity. In Lee et al.'s work [18],

X. Guo · Z. Qin · W. Fan · G. Wang · R. Zhao · S. Peng ·  
J. Wang (✉)  
State Key Laboratory of Coal Conversion, Institute of Coal  
Chemistry, Chinese Academy of Sciences, Taiyuan 030001,  
People's Republic of China  
e-mail: iccgw@sxicc.ac.cn

X. Guo  
Graduate University of the Chinese Academy of Sciences,  
Beijing 100049, People's Republic of China

the surfaces of MCM-41 and silica gel were functionalized with amino groups and then  $(VO)^{2+}$  ions were immobilized by covalent bonding with the multiple amino groups. The grafted vanadium metals showed high activity and leached only slightly from the solid MCM-41- $NH_2$ -(VO) in benzene hydroxylation. Andrew et al. [19] reported a novel heterogeneous catalyst based on a chemically modified mesoporous silica gel with immobilised cobalt ions: cyanide-functionalized mesoporous silica gel was treated with sulfuric acid and then  $Co^{2+}$  ions were introduced into the solid material by ion-exchange. The catalyst containing immobilized cobalt ions was successfully applied to the epoxidation of alkenes. All these propose that  $Pb(OAc)_2$ ,  $Zn(OAc)_2$  and  $Yb(OTf)_3$  hydrate immobilized on the mesoporous materials may provide ideal heterogeneous catalysts for the synthesis of carbamates from dialkyl carbonate and amines. SBA-15 with larger pore size and higher thermal stability compared with other mesoporous silica [20] may serve as ideal support for preparing such functionalized catalysts.

In this work, zinc carboxylate groups  $-COO(Zn)$  were grafted onto the pore surface of mesoporous SBA-15. FT-IR and NMR were used to characterize the carboxylate group immobilised on SBA-15. The mesoporous SBA-15 functionalized with zinc carboxylate was then used as a heterogeneous catalyst for the selective synthesis of MDC from DMC and MDA. The effects of reaction conditions on the MDC yield as well as the role of Lewis acid from zinc carboxylate groups in the catalytic performance were investigated.

## 2 Experimental

### 2.1 Catalyst Preparation

The preparation procedures of ordered mesoporous silica SBA-15 functionalized with carboxylate groups were similar to those reported by Yang et al. [21]. Briefly, 4 g of Pluronic 123 ( $EO_{20}PO_{70}EO_{20}$ ,  $M_{av} = 5,800$ , purchased from Acros Organics) was dissolved in 105.2 g of deionized water at 40 °C by stirring, and then 24.42 g of hydrochloric acid (37 wt%) was added. After that, tetraethyl orthosilicate (TEOS) was added dropwise in the solution and kept at 40 °C for 1 h, and then a certain amount of 3-cyanopropyltriethoxysilane (CPTES, Acros Organics) was slowly added. The molar composition of the mixture was  $(1 - x/100)$  TEOS :  $(x/100)$  CPTES:6.1 HCl:0.017 P123:165  $H_2O$ , where  $x = (CPTES/(TEOS + CPTES)) \times 100$  varied from 0 to 20. The mixture was stirred at 40 °C for 20 h; then it was transferred into a Teflon-lined autoclave and heated to 90 °C under static condition for 24 h. After that, the solid stuff from the

autoclave was filtered off, washed with deionized water, and dried at 80 °C for 12 h. In this way, SBA-15 grafted with  $-CN$  group was obtained.

To remove the template and to hydrolyze the  $-CN$  groups, 1.0 g of SBA-15 grafted with  $-CN$  group was redispersed in 120 mL of 48%  $H_2SO_4$  solution and heated to 95 °C for 24 h. The product was washed with water until the eluent became neutral, then it was dried at 80 °C for 24 h to get carboxylate-functionalized SBA-15 (denoted as CA/SBA-15- $x$ ).

Finally, 1.0 g of CA/SBA-15- $x$  was mixed with 50 mL of 0.1 M  $ZnCl_2$  aqueous solution and stirred for 6 h for ion-exchange of  $H^+$  with  $Zn^{2+}$ , and then the solid product was washed with water until no chloride ion was detected in the eluent. The resultant materials after the ion-exchange were dried at 80 °C for 12 h to obtain the zinc carboxylate functionalized SBA-15 (denoted as ZC/SBA-15- $x$ ). Si/Zn ratio could be determined by inductively coupled plasma-atomic emission spectrometry (ICP-AES).

For comparison, ZnAPO-5 ( $w(Zn) = 5\%$ ) was synthesized following a procedure described by Gómez-Hortigüela et al. [22]. ZnO/SBA-15 ( $w(Zn) = 4\%$ ) was prepared with aqueous  $Zn(NO_3)_2$  solution by a conventional impregnation method.

### 2.2 Catalyst Characterization

X-ray powder diffraction (XRD) patterns were collected on a Rigaku D Max III VC diffractometer using Cu  $K\alpha$  radiation ( $\lambda = 1.5404 \text{ \AA}$ ) at 40 kV and 20 mA in the  $2\theta$  range of 0.5° to 6°.

Nitrogen adsorption-desorption isotherms were measured by using Micromeritics Tristar 3000 gas absorption analyzer at 77.4 K. Before each measurement, the samples were degassed at 80 °C and  $10^{-4}$  Pa overnight. The specific surface area was calculated by the BET method and the pore size distribution was calculated from the desorption isotherms by the Barrett-Joyner-Halenda (BJH) method.

Transmission electron microscopy (TEM) was performed on a JEOL JEM2010 electron microscope, operated at an acceleration voltage of 200 kV.

Fourier transform infrared spectroscopy (FT-IR) was carried on a Nicolet 380 FT-IR Spectrometer with a resolution of  $2 \text{ cm}^{-1}$ .

The catalyst acidity was measured on a Nicolet Magna-IR 560 Spectrometer through pyridine adsorption. The samples in self-supporting wafers were first evacuated in the IR cell at 150 °C for 8 h, and then IR background spectra were recorded after the samples were cooled down to room temperature. After that, pyridine was admitted into the IR cell and the IR spectra of adsorbed pyridine were recorded after a degassing process at 150 °C for 2 h.

$^{13}\text{C}$  CP MAS NMR spectra were recorded on an Infinityplus-300 instrument at 75.4 MHz with a 2 s pulse delay using 7.5 mm zirconia rotors at a spinning speed of 1.5 kHz.

### 2.3 Catalytic Tests and Analytical Procedures

The catalytic reactions were carried out in a 20 mL stainless steel autoclave equipped with a magnetic stirrer. In a typical test, 2.52 mmol of MDA and 0.100 g of catalyst were first added into the autoclave, and then the autoclave was sealed and evacuated with a vacuum pump. After that, 4.54 mL of DMC was then charged into the autoclave through a syringe. The reaction was carried out under autogeneous pressure (about 1.0 MPa) at 170 °C for 4 h.

After reaction, the catalyst was separated by filtration. The products were analyzed by using an Agilent 1100 high performance liquid chromatography (HPLC) equipped with a column of Zorbax Eclipse XDB-C18 (4.6 × 150 mm) and an UV detector.

## 3 Results and Discussion

### 3.1 Crystalline Structure and Textual Properties of CA/SBA-15 and ZC/SBA-15

XRD patterns of CA/SBA-15 and its derivative ZC/SBA-15 after  $\text{Zn}^{2+}$  ion-exchanging are shown in Fig. 1. All samples show one intense peak of (100) and two weak diffraction peaks of (110) and (200). The XRD patterns of ZC/SBA-15 are coincident with those of CA/SBA-15, indicating that the crystallographic order of mesopores is preserved after the ion-exchange with  $\text{Zn}^{2+}$ . The well-resolved (110) and (200) reflections for the samples of

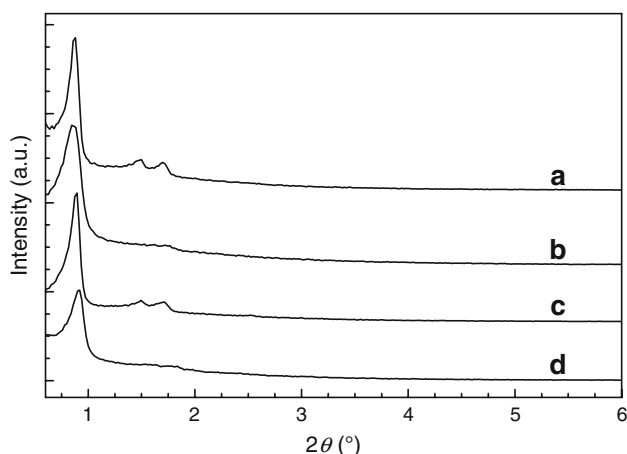


**Fig. 1** XRD patterns of the catalyst samples (a) CA/SBA-15-10, (b) CA/SBA-15-20, (c) ZC/SBA-15-10, (d) ZC/SBA-15-20

$x = 10$  reveal highly ordered mesopores in the SBA-15 materials. However, when  $x = 20$ , the reflections (110) and (200) are less resolved and less intense, showing that the mesoporous order decreases with the increase of CPTES usage. CPTES of high concentration may disturb the self-assembly of surfactant micelles and the silica precursor [16].

The nitrogen adsorption-desorption isotherms of CA/SBA-15 and ZC/SBA-15 are shown in Fig. 2a. The isotherms are of type IV with a narrow hysteresis loop indicating the existence of mesoporous structure [21]. The position of hysteresis loops shifts slightly to lower relative pressure and the step becomes less steep with the increase of CPTES content in the synthesis gel; this indicates that CA/SBA-15-10 (or ZC/SBA-15-10) has a larger pore size and a narrower distribution than CA/SBA-15-20 (or ZC/SBA-15-20), as shown in Fig. 2b.

The detailed pore structure parameters are summarized in Table 1. With the increase of cyanopropyl groups introduced into the mesoporous silicas, the pore diameter, surface area and pore volume of CA/SBA-15 and ZC/SBA-15 decrease obviously. These may be attributed to the

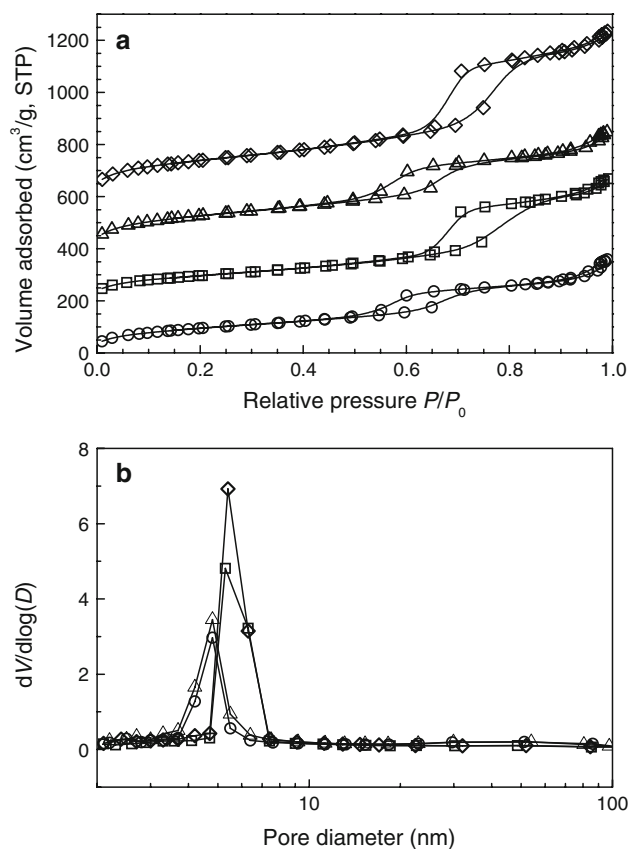


**Fig. 2** Nitrogen adsorption-desorption isotherms (a, from down to upper, shifted by 0, 250, 500 and 750  $\text{cm}^3 \text{g}^{-1}$  STP, respectively) and pore size distribution (b) of the samples:  $\diamond$ , CA/SBA-15-10;  $\Delta$ , CA/SBA-15-20;  $\square$ , ZC/SBA-15-10 and  $\circ$ , ZC/SBA-15-20

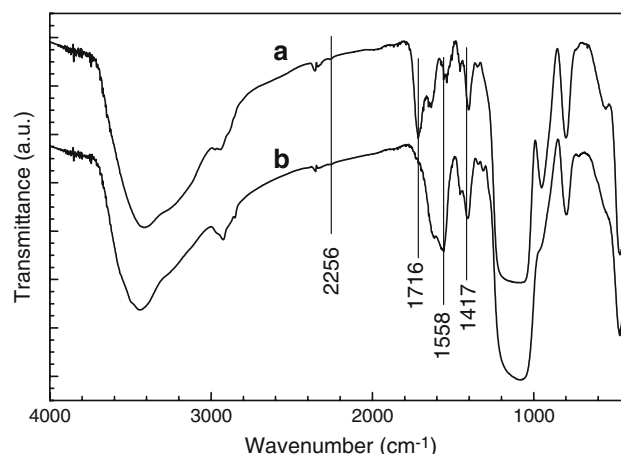
**Table 1** Textural properties of CA/SBA-15 and ZC/SBA-15 samples

Sample	D <sub>100</sub> spacing (nm)	Pore diameter (nm)	Surface area (m <sup>2</sup> /g)	Pore volume (cm <sup>3</sup> /g)	Si/Zn ratio	Total acidity (mmol/g)
CA/SBA-15-10	9.61	5.42	553.30	0.93	—	0.35
CA/SBA-15-20	9.58	4.79	469.99	0.69	—	0.72
ZC/SBA-15-10	9.59	5.33	424.01	0.78	20.59	0.39
ZC/SBA-15-20	9.54	4.78	350.18	0.56	14.90	0.78

occupation of large organic molecules in the pores as well as the disturbance of cyanopropyl groups during the silicate condensation process [15]. When Zn<sup>2+</sup> ions are coordinated on the surface of CA/SBA-15, a reduction of the surface area by about 25% is observed. This is probably due to that Zn<sup>2+</sup> ions dispersed in SBA-15 occupy parts of the channel pores [19]. However, the acidity of carboxylate functionalized SBA-15 seems to be proportional to the amounts of carboxylate incorporated in the SBA-15 framework.

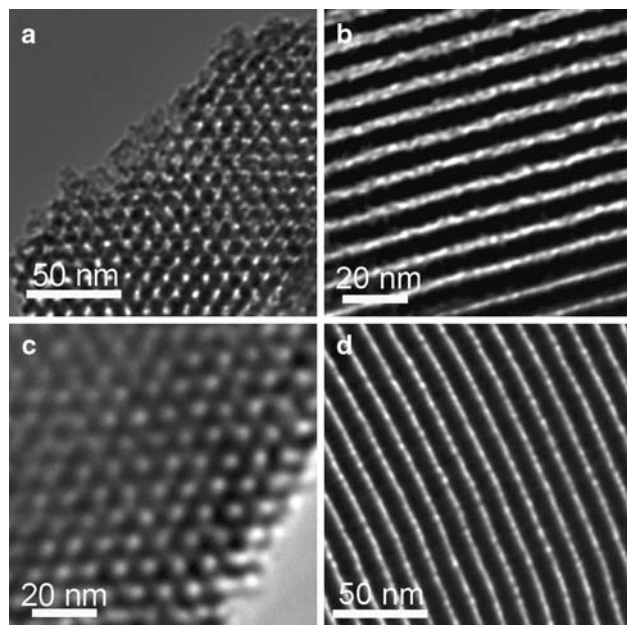
Figure 3 shows the TEM images of CA/SBA-15-10 and ZC/SBA-15-10. The well-ordered arrays of mesochannels indicate a typical two-dimensional *p6mm* hexagonal symmetry [23]. TEM images of ZC/SBA-15-10 show that the uniformly ordered mesoporous structure of SBA-15 is preserved after the ion-exchange with Zn<sup>2+</sup>.

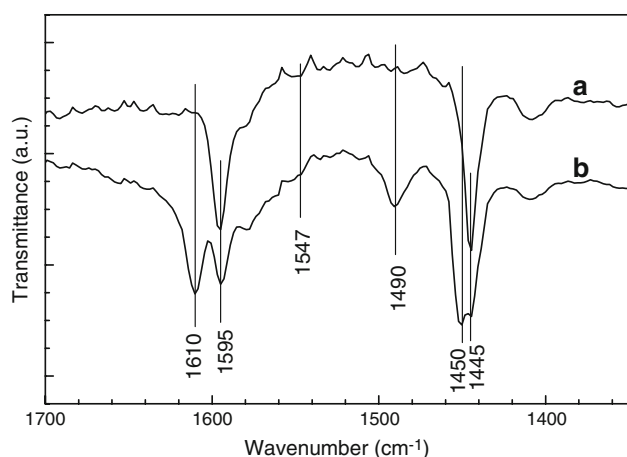
Figure 4 gives the infrared spectra of CA/SBA-15-10 and ZC/SBA-15-10. The absorption peak at 1,716 cm<sup>-1</sup> for CA/SBA-15-10 (line a) is typical C=O stretching vibration of carboxylic acid. The stretching vibration of -CN at

**Fig. 4** FT-IR spectra of (a) CA/SBA-15-10 and (b) ZC/SBA-15-10

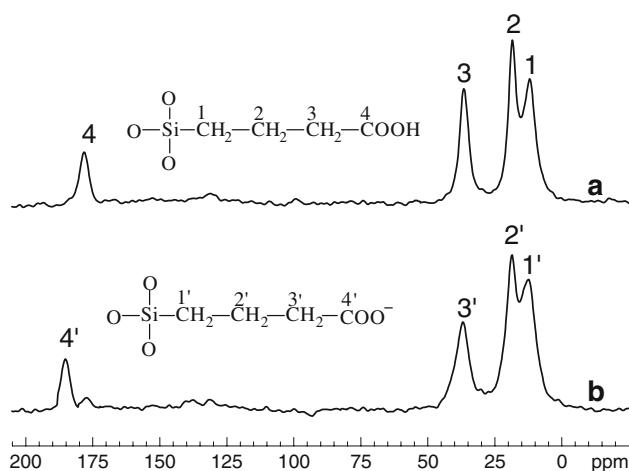
2,256 cm<sup>-1</sup> is not found, indicating that almost all -CN groups are hydrolyzed to -COOH upon the treatment with sulfuric acid [24]. With regard to ZC/SBA-15-10 (line b), two bands at 1,558 cm<sup>-1</sup> and 1,417 cm<sup>-1</sup> assigned to the asymmetric and symmetric stretching vibration of zinc carboxylate are observed along with the disappearance of C=O vibration peak at 1,716 cm<sup>-1</sup>. This indicates that the -COOH groups on the surface of SBA-15 are almost completely converted into the carboxylate -COO(Zn). The frequency separation of the asymmetric and symmetric COO<sup>-</sup> stretches for 141 cm<sup>-1</sup>, indicating that zinc carboxylate on ZC/SBA-15 is in bidentate coordination mode [25–27].

Figure 5 shows the FT-IR spectra of pyridine adsorbed on CA/SBA-15 and ZC-SBA-15 in the range of 1,700–1,350 cm<sup>-1</sup>. CA/SBA-15 (line a) gives the bands at 1,445 cm<sup>-1</sup> and 1,595 cm<sup>-1</sup> assigned to hydrogen bonded pyridine; the characteristic peaks of Brønsted acid sites (1,547 cm<sup>-1</sup>) and Lewis acid sites (1,450 cm<sup>-1</sup>) are not observed. However, ZC-SBA-15 (line b) exhibits the characteristic bands of pyridine adsorbed on Lewis acid sites at about 1,450 and 1,610 cm<sup>-1</sup>. Moreover, there is a band at 1,490 cm<sup>-1</sup> assignable to pyridine adsorption associated with both Lewis and Brønsted acid sites, while no peak of pyridine adsorbed on Brønsted acid sites (1,547 cm<sup>-1</sup>) is found [28]. This indicates that ZC-SBA-15 serves as a catalyst dominated by Lewis acidic sites.

**Fig. 3** TEM images of CA/SBA-15-10 (a and b) and ZC/SBA-15-10 (c and d) viewed from perpendicular direction (a and c) and parallel direction (b and d)



**Fig. 5** FT-IR spectra of pyridine adsorption on (a) CA/SBA-15-10 and (b) ZC/SBA-15-10



**Fig. 6**  $^{13}\text{C}$  CP/MAS-NMR spectra of (a) CA/SBA-15-10 and (b) ZC/SBA-15-10

The successful incorporation of CPTES in the carboxylate functionalized SBA-15 is further confirmed by  $^{13}\text{C}$  CP-MAS-NMR spectroscopy, as shown in Fig. 6.

$^{13}\text{C}$  CP-MAS NMR spectrum of CA/SBA-15-10 (line a) displays clearly four sorts of carbon with chemical shifts of  $\delta = 12.1$  ppm [29], 18.4 ppm, 36.5 ppm, and 178.6 ppm [30]; confirming that SBA-15 material is functionalized with  $-\text{COOH}$  groups. Besides, the peaks corresponding to the surfactant P123 in the range of 67–77 ppm are not observed, implying that the surfactant is removed by the treatment with concentrated sulfuric acid [15].  $^{13}\text{C}$  CP/MAS NMR spectrum of ZC/SBA-15-10 (line b) exhibits clearly four peaks at 12.5 ppm, 18.7 ppm, 37.0 ppm, and 184.5 ppm, corresponding to the C atoms in the  $\text{Si}-\text{CH}_2-\text{CH}_2-\text{CH}_2-\text{COO}^-$  group in sequence from left to right; the peaks at 178.6 ppm corresponding to  $-\text{COOH}$  is hardly observed. These suggest that the carboxyl  $-\text{COOH}$  groups are almost completely converted into the carboxylate  $-\text{COO}(\text{Zn})$  after ion-exchange with  $\text{Zn}^{2+}$ .

### 3.2 Catalytic Performance of Zinc Carboxylate Functionalized SBA-15

The reaction results of MDA methoxycarboxylation with DMC using different catalysts are presented in Table 2. No target product (MDC) is observed at 170 °C in the absence of catalyst (entry 1), indicating that a catalyst is essential for the formation of MDC under these conditions. CA/SBA-15 exhibits hardly any activity for MDC formation but brings on some side products like 4-(4-aminobenzyl)-*N*-methylaniline (entry 2). However, zinc carboxylate functionalized SBA-15 (ZC/SBA-15-10/20, entries 3, 4, 7–9) exhibits excellent catalytic performance in the synthesis of MDC from MDA and DMC. The catalytic performance of ZC/SBA-15-20 (entry 4) was equivalent to that of ZC/SBA-15-10 (entry 3). These suggested that the catalytic performance of ZC/SBA-15 depended on both the zinc content in ZC/SBA-15 and the integrality of mesoporous structure. The mesopore ordering decreases with the increase of the zinc carboxylate amounts in the catalyst. Higher Zn content does not give better catalytic results.

**Table 2** Catalytic activities of various catalysts for the methoxycarbonylation of MDA with DMC

Entry	Catalyst	Temperature (°C)	MDA conversion (%)	MAC yield (%)	MDC yield (%)	Others (%)
1	None	170	3.8	0	0	3.8
2	CA/SBA-15-10	170	2.2	0.4	0	1.8
3	ZC/SBA-15-10	170	100.0	6.8	86.5	6.7
4	ZC/SBA-15-20	170	99.1	7.5	87.3	4.3
5	ZnAPO-5	170	4.3	0	0	4.3
6	ZnO/SBA-15	170	4.1	0	0	4.1
7	ZC/SBA-15-10	130	31.6	30.4	0	1.2
8	ZC/SBA-15-10	150	75.2	46.9	23.6	4.7
9	ZC/SBA-15-10	180	100.0	4.4	87.8	7.8

Reaction conditions: 2.52 mmol MDA, 4.54 mL DMC, 0.1 g catalyst, reaction time 4 h ( $w(\text{Zn})$  of ZC/SBA-15-10 is 3.9%,  $w(\text{Zn})$  of ZnO/SBA-15 is 4%)



The yield of MDC over ZC/SBA-15-10 is equivalent to that with corresponding homogeneous catalyst [10]. On the other hand, other Zn-containing catalysts ZnAPO-5 and ZnO/SBA-15 do not show any activity in the methoxycarbonylation (entries 4 and 5). These suggest strongly that the activity of ZC/SBA-15 is ascribed to the coordination of carboxylate ligands to zinc cations.

The effects of reaction temperature on the methoxycarbonylation were also examined with ZC/SBA-15-10 as catalyst (Table 2, entries 3, 7–9). For an endothermic reaction, MDA conversion increases with the reaction temperature. At a temperature below 150 °C (entries 7 and 8), the reaction produces mainly the intermediate product mono-carbamate methyl-4-(4'-aminobenzyl)phenylcarbamate (MAC) via the reaction (1). At 170 °C (entry 3), MDA conversion reaches almost 100% and MDC yield reaches 86.5%. With further increasing the reaction temperature up to 180 °C (entry 9), MDC yield is in the same level. Therefore, a temperature of 170–180 °C is proper for MDA methoxycarbonylation with DMC to produce MDC over ZC/SBA-15; higher temperature may bring on serious side reactions and speed up the loss of active components.

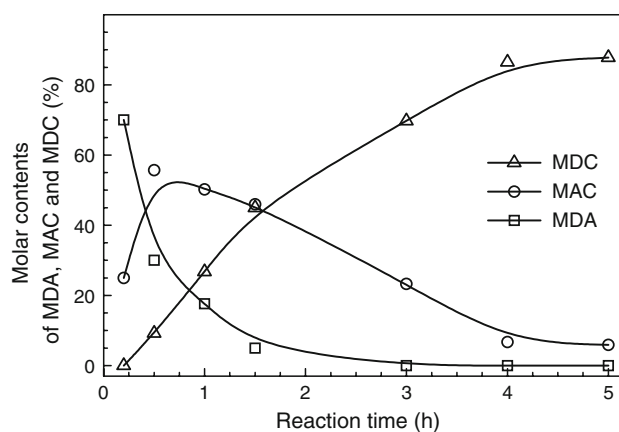


**Fig. 7** Dependence of MDA, MAC, and MDC contents in the reacting mixture on the reaction time (Reaction conditions: 2.52 mmol MDA, 4.54 mL DMC, 0.1 g ZC/SBA-15-10, 170 °C)

catalysts before and after reaction indicate that the leaching of zinc during the catalytic reaction was negligible. This indicates that ZC/SBA-15 possesses a good stability against leaching of the active species, which is an important feature for a heterogeneous catalyst system with immobilized active components. The slight decrease of

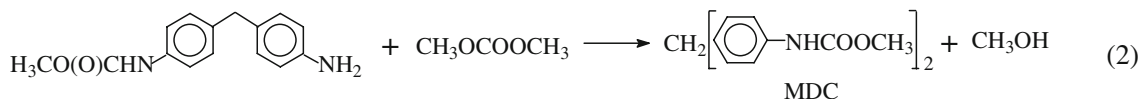
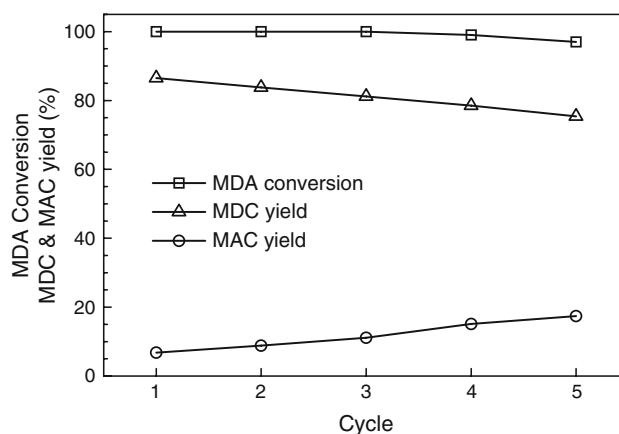
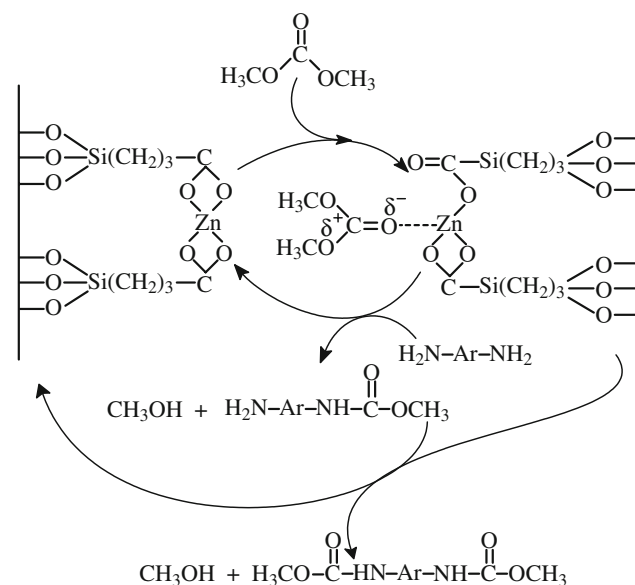


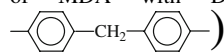
Figure 7 shows the effects of reaction time on MDA conversion and MDC yield over ZC/SBA-15-10. MAC content first increases with the reaction time, reaches a maximum after 0.75 h and then decreases with further increasing the reaction time. However, MDC yield increases with the reaction time and reaches a stable value after reaction for 4 h. This result suggests that the methoxycarbonylation of DMC and MDA is a consecutive process, as represented by reactions (1) and (2).

The recyclability of ZC/SBA-15-10 catalyst was examined under the same conditions. After each catalytic test, the solid catalyst was separated from the reaction medium by filtration, and then washed with ethanol and dried at 80 °C for 12 h. As shown in Fig. 8, ZC/SBA-15-10 catalyst can be reused without apparent decrease of its activity for 5 cycles. The elemental analyses of the



**Fig. 8** Stability of ZC/SBA-15-10 upon catalyst recycling (Reaction conditions: 2.52 mmol MDA, 4.54 mL DMC, 0.1 g ZC/SBA-15-10, 170 °C)



**Scheme 1** Proposed mechanism for the methoxycarbonylation of MDA with DMC over ZC/SBA-15 catalyst (Ar, )

catalytic activity upon catalyst recycling may be partially ascribed to the adsorption of organic species in the catalyst [31].

Based on above observations, a reaction mechanism for the methoxycarbonylation of MDA with DMC on ZC/SBA-15 is proposed, as illustrated in Scheme 1. First, the supported zinc carboxylate species as Lewis acid enhance the polarization of the carbonyl group in DMC. At the same time, the transformation of zinc carboxylate from bidentate coordination to monodentate coordination possibly causes the coordination of DMC with  $\text{Zn}^{2+}$ , thereby activating the carbonyl groups of DMC. After that, the amino group of MDA interacts with the carbonyl group of activated DMC, which creates the product and simultaneously restores the catalyst.

#### 4 Conclusions

The zinc carboxylate functionalized mesoporous SBA-15 (ZC/SBA-15) was prepared in three steps: first, SBA-15 grafted with  $-\text{CN}$  group was synthesized by the conventional one-pot route; then the  $-\text{CN}$  group was hydrolyzed into  $-\text{COOH}$  group in  $\text{H}_2\text{SO}_4$  solution; lastly,  $\text{Zn}^{2+}$  ions were introduced by a facile ion-exchange process. The immobilization of carboxylate group  $-\text{COO}(\text{Zn})$  on SBA-15 were confirmed by FT-IR and NMR characterizations.

ZC/SBA-15 as a heterogeneous catalyst exhibits excellent performance (high MDC yield and good recyclability) in the selective synthesis of MDC from DMC and MDA. The activity of ZC/SBA-15 may be ascribed to the coordination of carboxylate ligands to zinc cations. This provides a potential approach for the non-phosgene synthesis of isocyanates.

**Acknowledgments** The authors are grateful for the financial support of the State Key Fundamental Research Project (2006CB202504) and the Natural Science Foundation of China (20676140) and Shanxi Province (No. 051154).

#### References

- Blencowe A, Clarke A, Drew MGB, Hayes W, Slark A, Woodward P (2006) *React Funct Polym* 66:1284
- Mason RW (2004) US Patent 6,781,010
- Tafesh AM, Weigung J (1996) *Chem Rev* 96:2035
- Leconte MP, Francois (1992) US Patent 5,117,036
- Gasparini M, Ragaini F, Cazzaniga C, Cenini S (2005) *Adv Synth Catal* 347:105
- Kim HS, Kim YJ, Lee H, Park KY, Lee C, Chin CS (2002) *Angew Chem Int Ed* 41:4300
- Aresta M, Dibenedetto A, Quaranta E (1998) *Tetrahedron* 54:14145
- Baba T, Kobayashi A, Kawanami Y, Inazu K, Ishikawa A, Echizen T, Murai K, Aso S, Inomata M (2005) *Green Chem* 7:159
- Fu Z, Ono Y (1994) *J Mol Catal* 91:399
- Baba T, Kobayashi A, Yamauchi T, Tanaka H, Aso S, Inomata M, Kawanami Y (2002) *Catal Lett* 82:193
- Curini M, Epifano F, Maltese F, Rosati O (2002) *Tetrahedron Lett* 43:4895
- Zhao X, Wang Y, Wang S, Yang H, Zhang J (2002) *Ind Eng Chem Res* 41:5139
- Margolese D, Melero JA, Christiansen SC, Chmelka BF, Stucky GD (2000) *Chem Mater* 12:2448
- Wang X, Lin KSK, Chan JCC, Cheng S (2005) *J Phys Chem B* 109:1763
- Grieken RV, Melero JA, Morales G (2006) *J Mol Catal A Chem* 256:29
- Wang X, Tseng YH, Chan JCC, Cheng S (2005) *Micropor Mesopor Mater* 85:241
- Carloni S, De Vos DE, Jacobs PA, Maggi R, Sartori G, Sartorio R (2002) *J Catal* 205:199
- Lee CH, Lin TS, Mou CY (2003) *J Phys Chem B* 107:2543
- Butterworth AJ, Clark JH, Walton PH, Barlow SJ (1996) *Chem Commun* 16:1859
- Zhao D, Huo Q, Feng J, Chmelka BF, Stucky GD (1998) *J Am Chem Soc* 120:6024
- Yang CM, Wang Y, Zibrowius B, Schüth F (2004) *Phys Chem Chem Phys* 6:2461
- Gómez-Hortigüela L, Pérez-Pariente J, Blasco T (2005) *Micropor Mesopor Mater* 78:189
- Zhao D, Feng J, Huo Q, Melosh N, Fredrickson GH, Chmelka BF, Stucky GD (1998) *Science* 279:48
- Fiorilli S, Onida B, Bonelli B, Garrone E (2005) *J Phys Chem B* 109:16725
- Johnson MK, Powell DB, Cannon RD (1981) *Spectrochim Acta A* 37:899

26. Kazuo N (1978) Infrared and Raman spectra of inorganic and coordination compounds. Wiley, New York
27. Zelenák V, Györyová K, Mlynarcík D (2002) Metal Based Drugs 8:269
28. Li Y, Zhang W, Zhang L, Yang Q, Wei Z, Feng Z, Can Li (2004) J Phys Chem B 108:9739
29. Yiu HHP, Wright PA, Botting NP (2001) J Mol Catal B Enzym 15:81
30. Chong ASM, Zhao XS, Kustedjo AT, Qiao SZ (2004) Micropor Mesopor Mater 72:33
31. Wang XG, Chen CC, Chen SY, Mou Y, Cheng S (2005) Appl Catal A Gen 281:47